NUMERICAL ANALYSIS OF THE IMPACT OF A VEGETATION FAÇADE ON THE IMMEDIATE SURROUNDINGS OF A BUILDING

Štěpánka Chomová*,1, Jan Vystrčil[1], Vojtěch Vaněk[1], David Bečkovský[1], Jan Pěnčík[1], Karel Šuhajda[1]

*chomova@vutbr.cz
[1]Faculty of Civil Engineering, Institute of Building Structures, Brno University of Technology, Veveří 331/95 602 00 Brno, Czech Republic

Abstract

This study evaluates the impact of a vegetation façade on the immediate surroundings of a residential building using numerical simulations. The analysis focuses on key thermal indicators, including Mean Radiant Temperature (MRT), Physiological Equivalent Temperature (PET), and Universal Thermal Climate Index (UTCI). The results demonstrate that implementing a vegetation façade can significantly reduce thermal stress in urban environments, with temperature reductions of up to 8°C in the affected area. These findings highlight the potential of green façades as an effective strategy for mitigating urban heat island effects and improving outdoor thermal comfort.

Keywords

Vegetation façade, urban heat island, thermal comfort, numerical simulation, green infrastructure

1 INTRODUCTION

Urban heat islands (UHI) are areas or zones within cities that exhibit significantly higher temperatures compared to their surrounding environments [1]. UHIs result from human urbanization, that is, human activities. The term urbanization describes two closely related phenomena. Firstly, it reflects the absolute and relative proportion of the population living in densely populated areas, primarily engaged in non-agricultural activities. Secondly, it refers to the transformation of natural landscapes into environments suitable for human activity. Changes in the environment caused by human activities—such as the construction of buildings, the conversion of natural surfaces into paved areas, the removal of vegetation, and modifications to watercourse designs—lead to the formation of a unique microclimate in the affected area. UHI is thus the expression of the temperature difference between a built-up urban area (or part of it) and the surrounding natural (non-urbanized) environment [2]

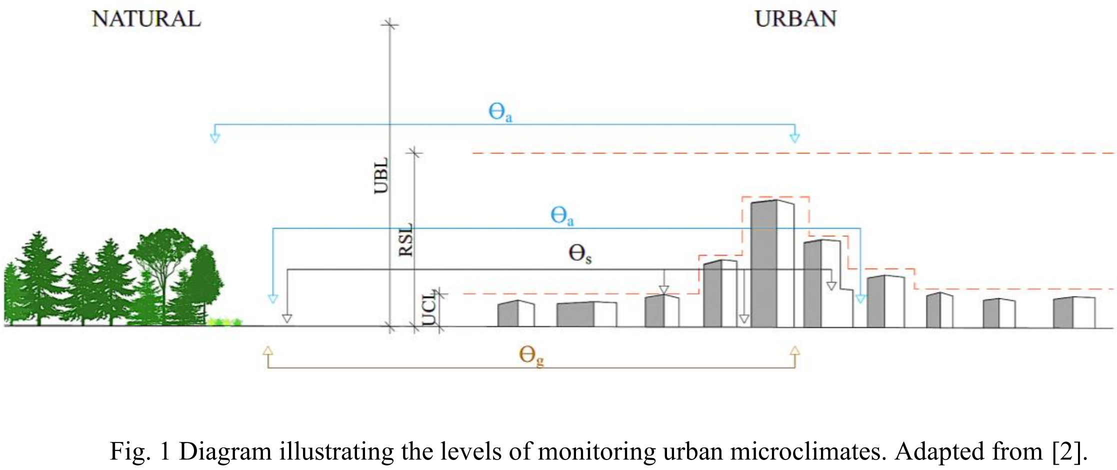

Fig. 1 Diagram illustrating the levels of monitoring urban microclimates. Adapted from [2].

In (Fig. 1), a diagram illustrating the possibilities for monitoring urban microclimates and the classification of Urban Heat Islands (UHI) is presented. According to [2], for monitoring microclimates, urbanized areas are divided into three vertical levels:

Received 12/03/2025/Accepted/Published 30/09/2025 DOI 10.13164/juniorstav.2025.26138

- UBL (Urban Boundary Layer): This layer encompasses the built-up area up to the atmospheric height above the roof level of buildings.
- RSL (Roughness SubLayer): A sublayer representing the roughness of the original surface.
- UCL (Urban Canopy Layer): A sublayer corresponding to the roof levels of the built-up area.

As shown in (Fig. 1), several temperature measurements are compared:

- Air temperature (Θ_a [°C]): Measured at a height far above the rooftops for climate monitoring.
- Air temperature (Θ_a): Measured in the human activity zone (1.3–2 m above ground level).
- Surface temperature (Θ_s): Measured on the surfaces of façades, roofs, roads, and pedestrian areas [2].

Ground temperature (Θ_g): Measured at the ground level.

Based on the location of temperature monitoring in urbanized areas, UHI can be classified into:

- Canopy-level UHI (CUHI): Monitored near the surfaces of buildings below roof level.
- Boundary-level UHI (BUHI): Monitored at the boundary of the urbanized area, above the building layers.
- Surface UHI (SUHI): Monitored at the surfaces of urban areas, including terrain, walls, and roofs.

Ground UHI (GUHI): Monitored at the subsurface layers of urban areas.

Most commonly, UHI are monitored in human activity zones (approximately 1.3–2 m above ground level – CUHI) and at the surfaces of building structures (SUHI). During the summer months, building surfaces experience significant temperature increases, which are subsequently transferred to the surroundings. According to [50], these elevated temperatures have a significant impact on the thermal comfort and health of urban residents.

Possibilities of numerical modelling and prediction of urban heat Islands

The first documented observations of the UHI phenomenon date back to the early 19th century in England, with temperature measurements conducted in London [3]. As scientific disciplines advanced, research on UHI formation and characterization expanded to large cities worldwide [4], [5], [6]. With the progression of climate change, UHI occurrences have become more frequent and their effects more pronounced [7], [8].

Efforts to mitigate UHI effects have evolved alongside the growing concern. In already urbanized problematic areas, mitigation measures include the addition of water features in public spaces, vegetation for shading and natural cooling, and the implementation of green roofs and walls [9], [10], [2], [11]. For new developments, considerations focus on environmental sustainability and user comfort in buildings, surrounding areas, and public zones.

For evaluation and design, numerical methods are employed to simulate the impact of buildings on their surroundings and quantify key parameters influencing the formation or reduction of UHIs. These methods include solar radiation analysis for specific locations, wind flow simulations using Computational Fluid Dynamics (CFD) [79], pedestrian-level thermal comfort assessments, and studies on rainwater utilization.

Over the past 40 years, significant advancements have been made in assessing thermal comfort. Expanding knowledge and increasing computational power now allow for the detailed analysis of urban areas in terms of thermal comfort. A wide range of computational models and indices are available to evaluate human thermal comfort. Tools such as CitySim Pro [12], ENVI-met [13], RayMan [14], Rhinoceros with Ladybug plugins [15], [16], Autodesk Forma [17], and SimScale [18] are commonly used.

In assessing outdoor thermal comfort, the level of thermal stress experienced by individuals is evaluated. Various indices have been developed to express thermal comfort, with globally recognized indices suitable for temperate climates, such as the Physiological Equivalent Temperature (PET) [19], [20], and the Universal Thermal Climate Index (UTCI) [19], [89]. These indices provide a detailed assessment of heat exchange between the human body and the surrounding environment, accounting for factors such as air temperature, solar radiation, wind speed, and relative humidity [19], [20], [21]. Both PET and UTCI are expressed in degrees Celsius (°C).

The UTCI is defined as the equivalent temperature at which the human body achieves the same physiological response as under actual climatic conditions. This equivalent approach involves comparing all other climatic conditions to a reference environment with assumed uniform physiological conditions based on the equivalence

DOI 10.13164/juniorstav.2025.26138

of dynamic physiological responses predicted by the model for both the actual and reference environments [89]. Calculating UTCI requires determining the body's thermal balance and comparing it to reference conditions, which include a wind speed measured at 10 m above ground, air temperature equal to mean radiant temperature, and relative humidity of 50%. UTCI provides a standardized scale for classifying environments and human thermal stress responses see at figure (Fig. 2).

Extreme cold stress	Very strong cold stress	Strong cold stress	Moderate cold stress	Mild cold stress	No thermal stress	Mild heat stress	Moderate heat stress	Strong heat stress	Extreme heat stress
< - 40 °C	-40 to -27 °C	-27 to -13 °C	-13 to 0 °C	0 to +9 °C	+9 to 26 °C	+ 26 to +32 °C	+ 32 to +38 °C	+ 38 to + 46 °C	> + 46 °C

Fig. 2 Display of categories of human response to ambient temperature expressed by the UTCI index. Taken from [21].

PET (Physiological Equivalent Temperature) is defined according to [20] as the physiologically equivalent temperature at any given location (outdoors or indoors) and corresponds to the air temperature at which the human body maintains thermal equilibrium in a typical indoor environment. This means that PET corresponds to the air temperature at which the human core and skin temperatures are the same as under the assessed conditions, assuming a work metabolism of 80 W (light activity) and a clothing thermal resistance of 0.9 clo.

Assumptions for the indoor reference climate:
- The mean radiant temperature equals the air temperature ($\Theta_{mrt} = \Theta_a$).
- Air velocity is set to 0.1 m·s^{-1}.
- Water vapor pressure is set to 12 hPa (approximately corresponding to a relative humidity of 50% at Θ_a = 20 °C).

Extreme cold stres	Very strong cold stress	Strong cold stress	Mild cold stress	No thermal stress	Mild heat stress	Strong heat stress	Very strong heat stress	Extreme heat stress

+4 °C	+ 8 °C	+13 °C	+18 °C	+23 °C	+29 °C	+35 °C	+41 °C	

Fig. 3 Display of categories of human response to ambient temperature expressed by the PET index. Taken from: [20].

DOI 10.13164/juniorstav.2025.26138

2 METHODOLOGY

In this chapter, the impact of installing a vegetative façade on a single-family house is analysed using numerical simulations in two model scenarios. In the first scenario, the model space was assessed without the use of a vegetative façade. In the second scenario, the model was supplemented with the vegetative façade surface.

For the numerical simulation of the influence of the vegetative façade on the building's surroundings, the Envi-met software in its student version was selected. The computational model includes boundary conditions for the atmospheric model, substrate, vegetation, and surfaces of the terrain and buildings. The document [22] describes the calculation methodology, relationships for individual boundary conditions, and the transfer of mass and energy.

Model Description

For the numerical simulation, a model was created based on a proposed scenario of a semi-detached house with a flat roof. One section of the building is considered single-story, while the other is two-story. The semi-detached house directly adjoins a sidewalk, followed by a strip of greenery and a roadway. The roadway continues with a green strip and a symmetrically designed sidewalk along its longitudinal axis. Near the semi-detached house, designated parking areas and green spaces representing a garden were incorporated into the model.

No trees or other tall vegetation exceeding 0.25 m in height were included in the model. The model was designed to clearly observe and define the impact of the vegetative façade on the building's immediate surroundings using numerical simulation. Additionally, it represents a section of a typical newly developed area where no landscape modifications were planned.

The model was created within a computational domain measuring 50 × 50 × 25 m, divided into square grid cells. The grid cell size was set to 1 m to balance calculation accuracy and computational time, which totalled 25 hours under the given settings. The semi-detached house has a ground plan dimension of 16 × 13 m, with the single-story and two-story sections each measuring 8 × 13 m. The height of the lower section is 4 m, while the higher section reaches 7 m.

Surface materials for the building structures and terrain were selected from the software library. The terrain materials include asphalt for roads, concrete paving for sidewalks, terraces, and parking areas, and clay-sandy soil for the substrate. The building envelope consists of masonry with an external thermal insulation system. The flat roof is designed as a single-layer structure with a grey-coloured waterproof membrane.

DOI 10.13164/juniorstav.2025.26138

Window and door openings, along with their glazing, were omitted due to the computational grid size and to optimize calculation time. The model space is illustrated in (

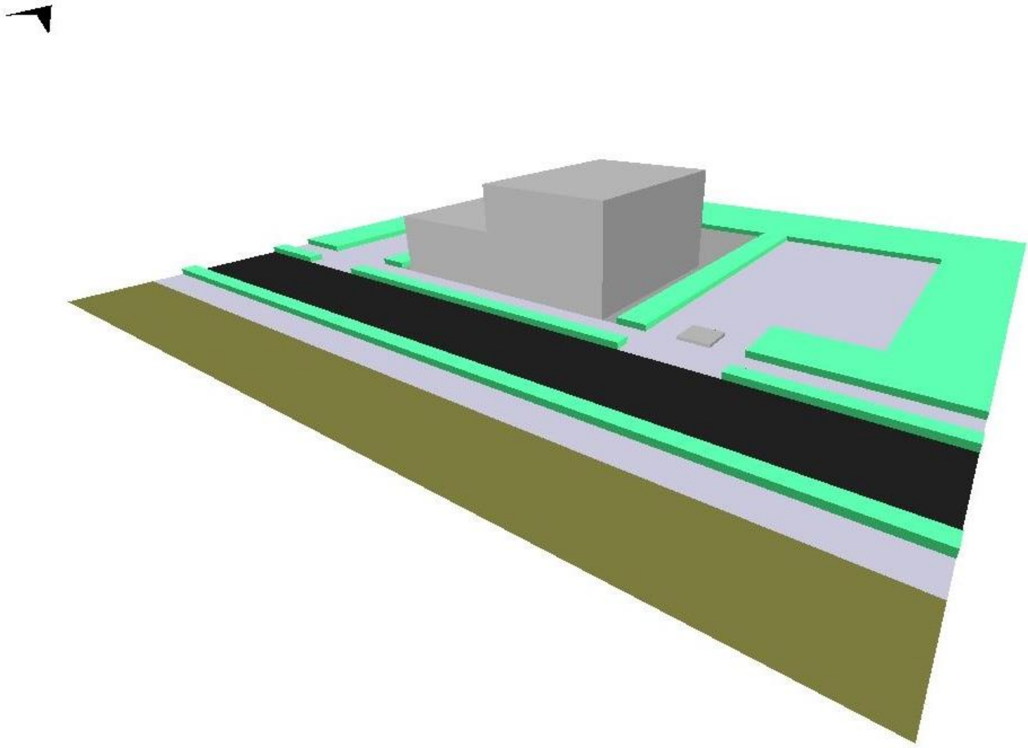

Fig. 4) and (Fig. 5).

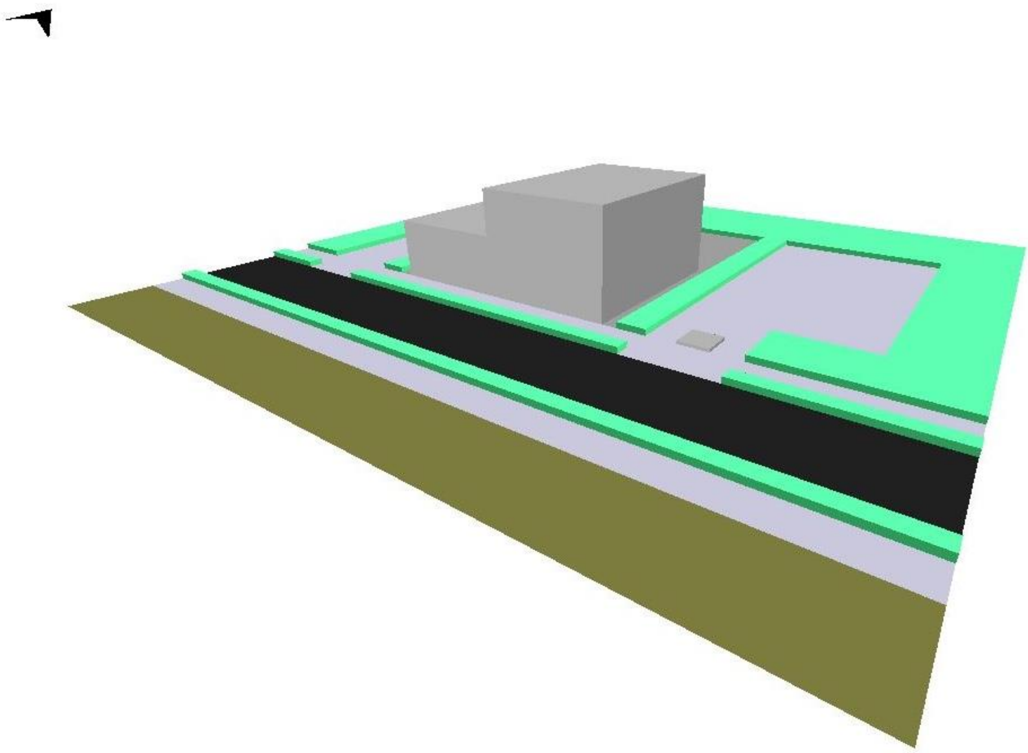

DOI 10.13164/juniorstav.2025.26138

Fig. 4 Axonometric view of the computational model with modification of areas for traffic routes, pedestrian areas, greenery and a placed semi-detached house object in the Envi-met software environment. Display of the model without placed vegetation façade.

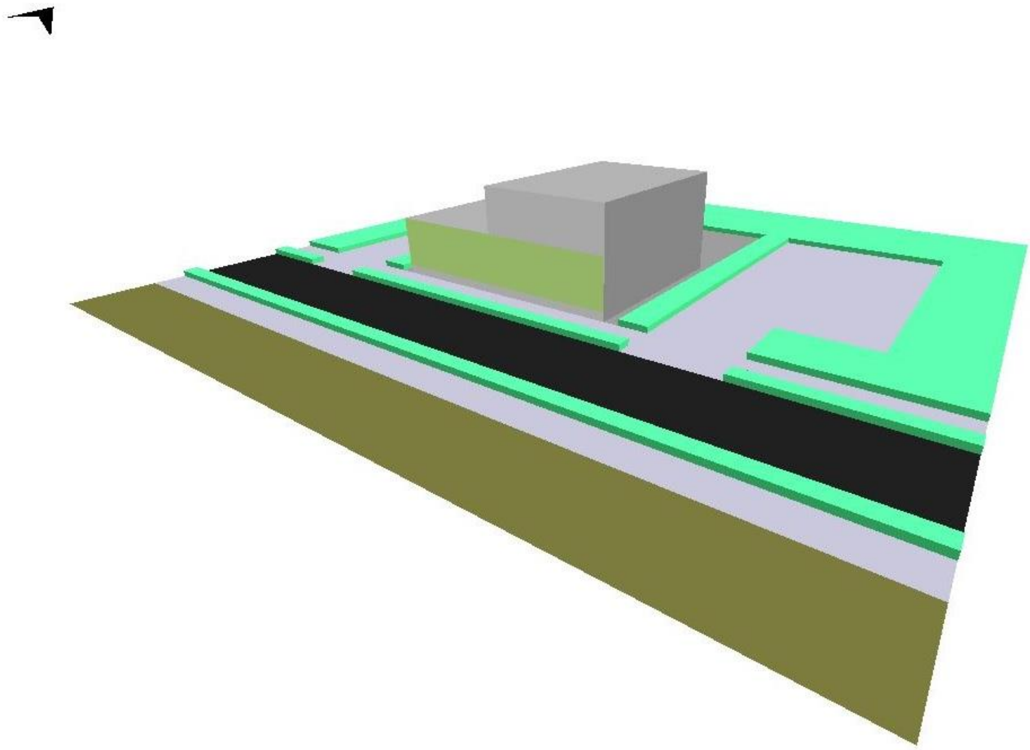

Fig. 5 Axonometric view of the computational model with modification of areas for traffic routes, pedestrian areas, greenery and a placed semi-detached house object in the Envi-met software environment. Display of the model with placed vegetation façade.

For the analysis to demonstrate the impact of the vegetative façade on the surroundings of the building, a vegetative façade was applied to the model of the semi-detached house within the height range of 0.5 m above ground level up to 4 m (the height of the lower section of the building). The vegetative façade was installed on the southern exterior wall of both buildings, specifically on the wall directly adjacent to the sidewalk.

Boundary Conditions for the Calculation

The simulation was initiated on August 22, 2023, at 5:00 AM, with a 24-hour simulation period. In the software, there are two methods for defining boundary climatic conditions for the calculation:

- Simplified input, where the user manually enters individual parameters into the software.
- Comprehensive input, where a file containing hourly recorded climatic data is imported.

For this simulation, the simplified input method was used. The software interface for entering climatic conditions is shown in **(**Figure 81**)**. The boundary climatic conditions were set as follows:

- Minimum daily air temperature**:** θ_air, min = 18°C at 6:00 AM
- Maximum daily air temperature**:** θ_air, max = 32°C at 2:00 PM
- Minimum relative humidity**:** φ_air, min = 43% at 5:00 AM
- Maximum relative humidity**:** φ_air, max = 92% at 2:00 PM
- Wind speed**:** v = 2 $m \cdot s^{-1}$
- Wind direction azimuth**:** 315°

Figure (Fig. 6) shows the input interface for setting the boundary climatic conditions for outdoor environment calculations.

DOI 10.13164/juniorstav.2025.26138

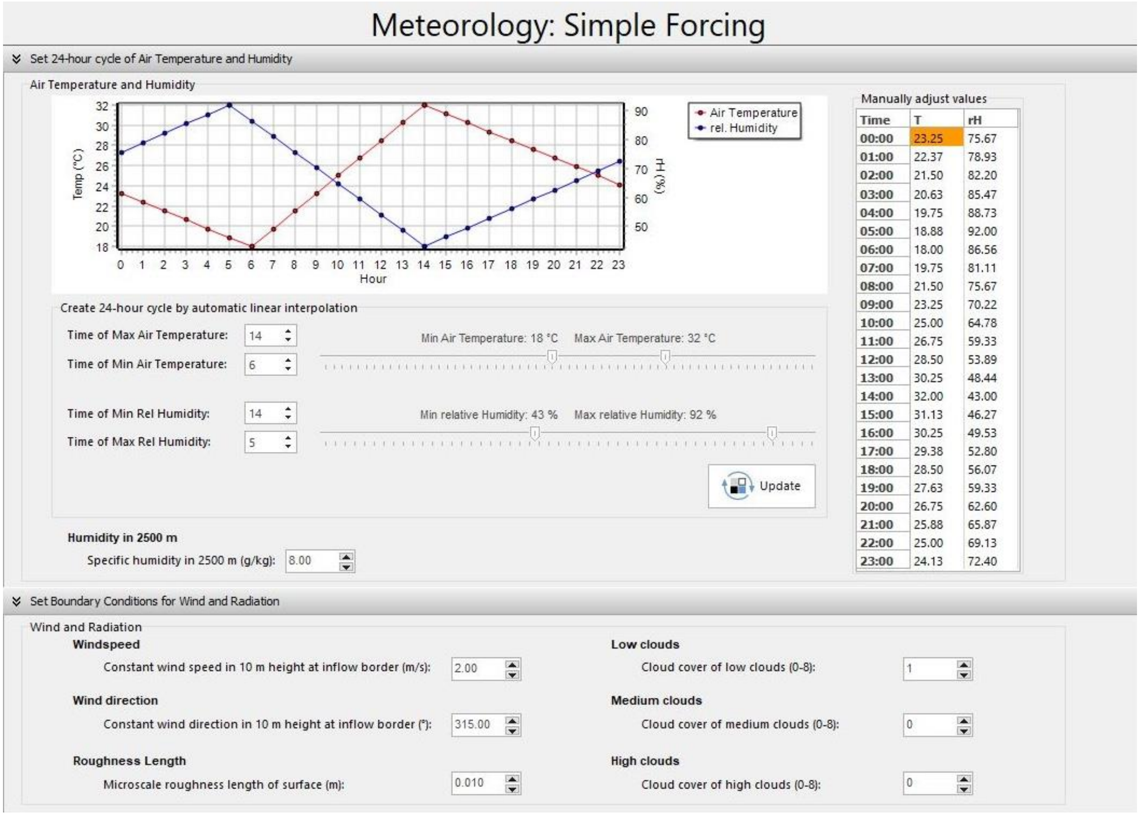

Fig. 6 Interface Envi-met software. Specific boundary climatic conditions for calculating outdoor environment parameters.

Analysis of Vegetation Façade Impact

The impact of the vegetation façade was assessed by analysing partial results and comparing them. From the available outputs generated by the software, the following key indicators are presented:

MRT (Mean Radiant Temperature) in a horizontal plane at the occupancy zone level (1.5 m above ground level)

PET (Physiological Equivalent Temperature) at the occupancy zone level (1.5 m above ground level)

UTCI (Universal Thermal Climate Index) at the occupancy zone level (1.5 m above ground level)

3 RESULTS

The results are presented in the form of temperature maps, which are placed in a horizontal plane at a height of 1.5 m above the ground, corresponding to the occupancy zone of the outdoor environment. The analysis results are interpreted at the times of the highest daily temperature increases, specifically at:

- 12:00 PM
- 3:00 PM
- 6:00 PM

To illustrate the impact of the vegetative façade on the thermal behavior of the model, the results are displayed in three columns:

- Column A – Model without a vegetative façade
- Column B – Model with a vegetative façade
- Column C – Absolute temperature difference between both scenarios (C = A – B)

The corresponding results are shown in Figures (Fig. 7 – Fig. 9).

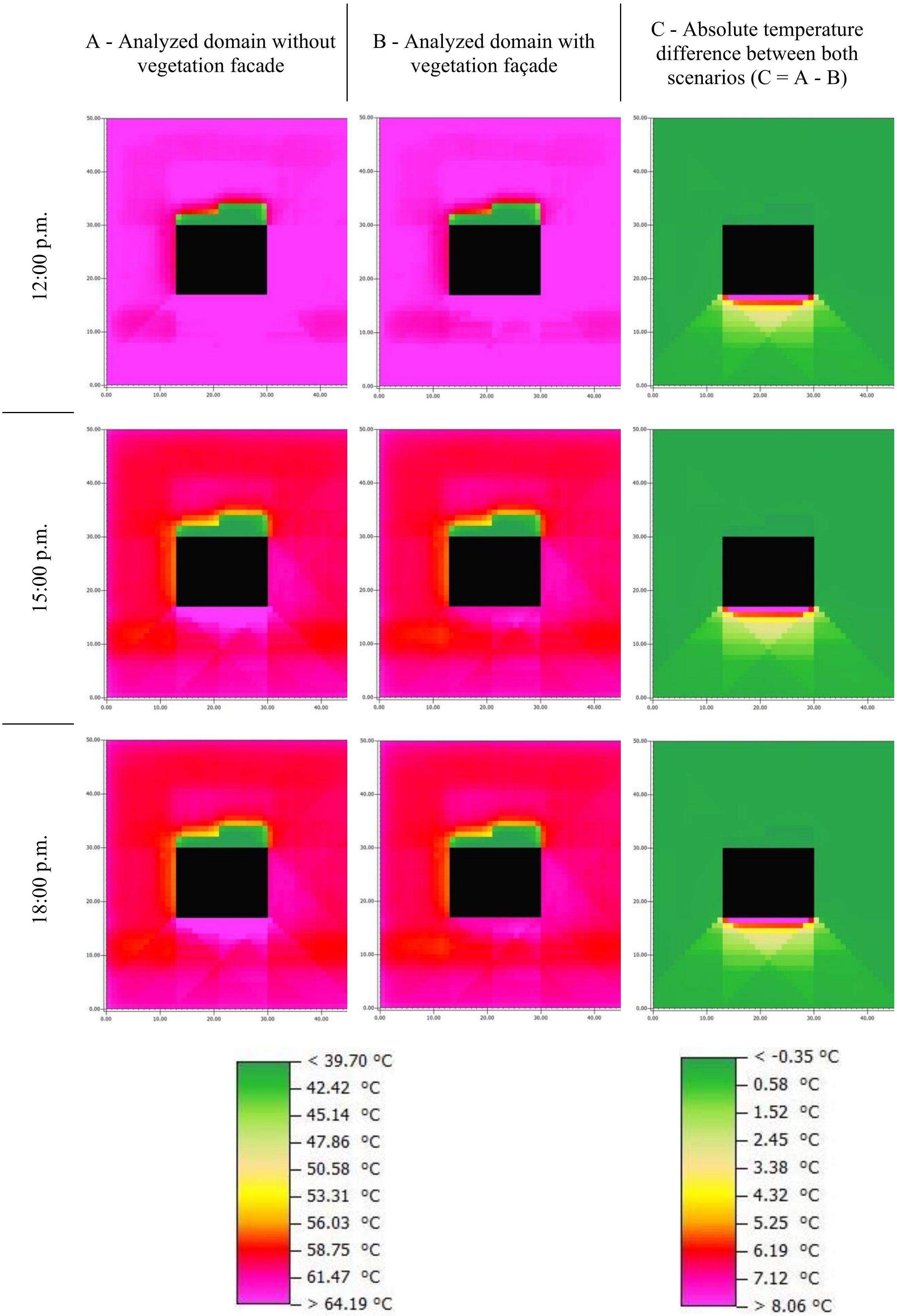

Fig. 7 Distribution of MRT (Mean Radiant Temperature) of the selected design situation (columns A and B) and their absolute difference for evaluating the impact of the vegetated facade on the building's surroundings (column C).

DOI 10.13164/juniorstav.2025.26138

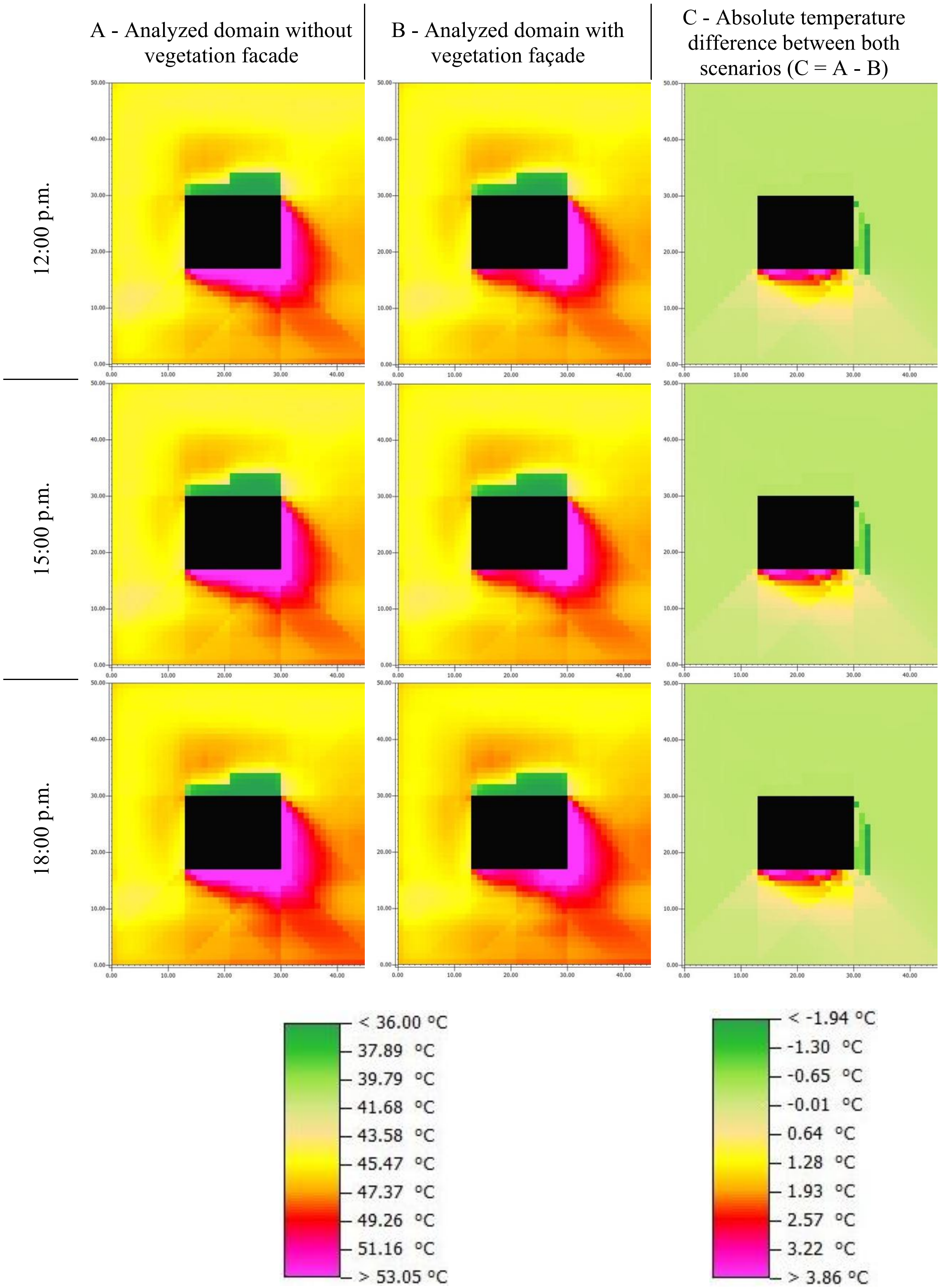

Fig. 8 Distribution of PET (Physiognomic Equivalent Temperature) of the selected design situation (columns A and B) and their absolute difference for evaluating the impact of the vegetated facade on the building's surroundings (column C).

DOI 10.13164/juniorstav.2025.26138

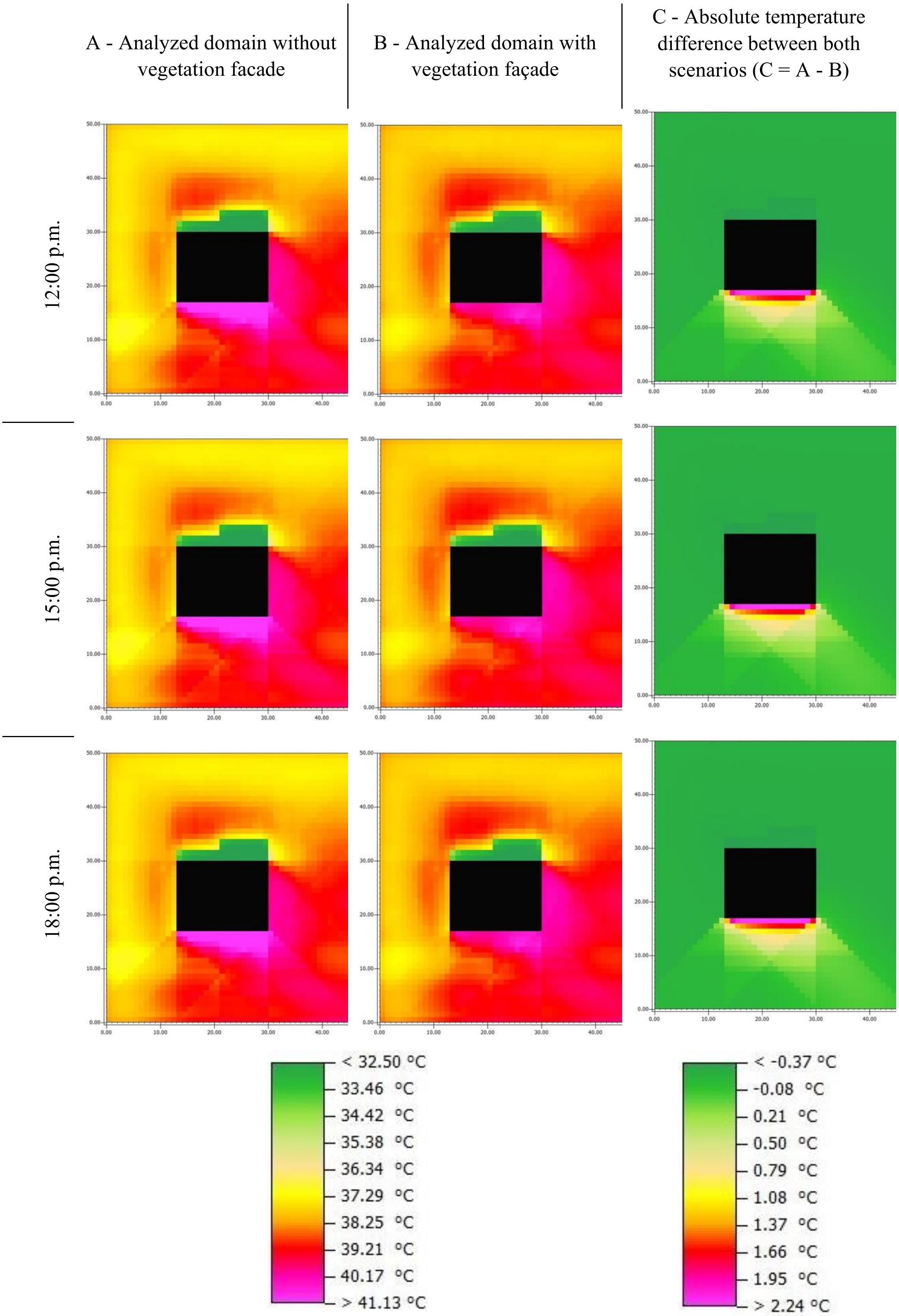

Fig. 9 Distribution of UTCI (Universal Thermal Climate Index) of the selected design situation (columns A and B) and their absolute difference for evaluating the impact of the vegetated facade on the building's surroundings (column C).

4 DISCUSSION

As part of the presented analysis and research, selected perceived temperature indices UTCI and PET were described. A comparison of numerical analysis results using these indices highlights differences in the impact of greenery on the perceived temperature within the analysed space.

For future research, in-situ measurements are planned, with a computational domain created to match the observed conditions. By evaluating and comparing measured and simulated data, it will be possible to validate and correlate the results.

The conducted analysis utilized basic material datasets available in the Envi-met software library. By comparing numerical simulation results with real-world measurements, library elements for green façades can be adjusted or expanded to improve accuracy.

Currently, more detailed libraries are used in Greenpass certification. However, the library elements employed for certification calculations are not publicly available.

5 CONCLUSION

To assess the impact of the vegetative façade based on the temperature maps in Figures 82, 83, and 84, Column C is the key indicator, as it represents the absolute temperature difference between the scenario without the vegetative façade and the one with it.

When evaluating the effect of the vegetative façade on temperature regulation around the building in terms of Mean Radiant Temperature (MRT), the simulation results (Figure 82) show a decrease in MRT by up to 8°C in front of the vegetative façade.

When evaluating the location using the Physiological Equivalent Temperature (PET) and Universal Thermal Climate Index (UTCI), the results indicate that perceived temperature is significantly influenced by environmental factors such as airflow, humidity, and human activity levels, rather than just Mean Radiant Temperature (MRT)alone.

When comparing the perceived temperature indices, the PET assessment shows more favourable results, indicating a greater cooling effect in front of the vegetative façade compared to the UTCI evaluation.

Acknowledgements

This paper was writhed with the financial support of specific university research project FAST VUT in Brno, No. FAST-S-23-8413 (2024).

References

[1] ROTH, M. -Urban Heat Islands. In: Handbook of Environmental Fluid Dynamics, Volume Two. CRC Press, 2012. p. 162-181.
[2] The Urban Heat Island, 2021. Online. Elsevier. ISBN 9780128150177. Available from: https://doi.org/10.1016/C2017-0-02872-0. [cit. 2025-03-12].
[3] MILLS, Gerald, 2008. Luke Howard and The Climate of London. Online. Weather. y. 63, v. 6, p. 153-157. ISSN 0043-1656. Available from: https://doi.org/10.1002/wea.195. [cit. 2025-03-12].
[4] ZHANG, Kaixuan; WANG, Rui; SHEN, Chenchen a DA, Liangjun, 2010. Temporal and spatial characteristics of the urban heat island during rapid urbanization in Shanghai, China. Online. Environmental Monitoring and Assessment. y. 169, v. 1-4, p. 101-112. ISSN 0167-6369. Available from: https://doi.org/10.1007/s10661-009-1154-8. [cit. 2025-03-12].
[5] YANG, Li; QIAN, Feng; SONG, De-Xuan a ZHENG, Ke-Jia, 2016. Research on Urban Heat-Island Effect. Online. Procedia Engineering. V. 169, p. 11-18. ISSN 18777058. Available from: https://doi.org/10.1016/j.proeng.2016.10.002. [cit. 2025-03-12].
[6] HEUSINKVELD, Bert G.; STEENEVELD, G. J.; VAN HOVE, L. W. A.; JACOBS, C. M. J. and HOLTSLAG, A. A. M., 2014. Spatial variability of the Rotterdam urban heat island as influenced by urban land use. Online. Journal of Geophysical Research: Atmospheres. 2014-01-27, roč. 119, č. 2, s. 677-692. ISSN 2169-

897X. Available from: https://doi.org/10.1002/2012JD019399. [cit. 2025-03-12].
[7] CHAPMAN, Sarah; WATSON, James E. M.; SALAZAR, Alvaro; THATCHER, Marcus a MCALPINE, Clive A., 2017. The impact of urbanization and climate change on urban temperatures: a systematic review. Online. Landscape Ecology. Y. 32, V. 10, p. 1921-1935. ISSN 0921-2973. Available from: https://doi.org/10.1007/s10980-017-0561-4. [cit. 2025-03-12].
[8] CORBURN, Jason, 2009. Cities, Climate Change and Urban Heat Island Mitigation: Localising Global Environmental Science. Online. Urban Studies. Year. 46, V. 2, p. 413-427. ISSN 0042-0980. Available from: https://doi.org/10.1177/0042098008099361. [cit. 2025-03-12].
[9] ENZI, V., B. CAMERON, P. DEZSÉNYI, D. GEDGE, G. MANN and U. PITHA. Nature-Based Solutions and Buildings: The Power of Surfaces to Help Cities Adapt to Climate Change and to Deliver Biodiversity. Kabisch N., Korn H., Stadler J., Bonn A. (eds), 2017. ISBN 978-3-319-53750-4.
[10] PASCHOALINO DE JESUS, Marina, Júlia M. LOURENÇO, Rosa M. ARCE a Manuel MACIAS. Green façades and in situ measurements of outdoor building thermal behaviour. Building and Environment [online]. 2017, 2017(119), 11-19 [cit. 2021-12-06]. Available from: https://www.sciencedirect.com/science/article/pii/S0360132317301506
[11] PERINI, Katia; OTTELÉ, Marc; FRAAIJ, A.L.A.; HAAS, E.M. a RAITERI, Rossana, 2011. Vertical greening systems and the effect on air flow and temperature on the building envelope. Online. Building and Environment. y. 46, v. 11, p. 2287-2294. ISSN 03601323. Available from: https://doi.org/10.1016/j.buildenv.2011.05.009. [cit. 2025-03-12].
[12] Citysim pro, 2010. Online. Available from: http://www.kaemco.ch/download.php. [cit. 2025-03-12].
[13] Envi-met, 2010. Online. Available from: https://envi-met.com. [cit. 2025-03-12].
[14] RayMan, 2010. Online. Available from: https://www.urbanclimate.net/rayman/. [cit. 2025-03-12].
[15] Rhinoceros, 2010. Online. Available from: https://www.rhino3d.com. [cit. 2025-03-12].
[16] Ladybug, 2018. Online. Available from: https://www.ladybug.tools. [cit. 2025-03-12].
[17] Autodesk forma, 2022. Online. Available from: https://www.autodesk.com/products/forma/overview?term=1-YEAR&tab=subscription. [cit. 2025-03-12].
[18] Simscale, 2015. Online. Available from: https://www.simscale.com. [cit. 2025-03-12].
[19] NABONI, Emanuele; MELONI, Marco; COCCOLO, Silvia; KAEMPF, Jérôme a SCARTEZZINI, Jean-Louis, 2017. An overview of simulation tools for predicting the mean radiant temperature in an outdoor space. Online. Energy Procedia. v. 122, p. 1111-1116. ISSN 18766102. Available from: https://doi.org/10.1016/j.egypro.2017.07.471. [cit. 2025-03-12].
[20] HÖPPE, P., 1999. The physiological equivalent temperature - a universal index for the biometeorological assessment of the thermal environment. Online. International Journal of Biometeorology. 1999-10-25, y. 43, v. 2, p. 71-75. ISSN 0020-7128. Available from: https://doi.org/10.1007/s004840050118. [cit. 2025-03-12].
[21] UTCI, 2012. Online. Available from: https://www.utci.org. [cit. 2025-03-12].
[22] Envi-met 3.0 overview, 2004. Online. Available from: https://www.envi-met.net/documents/papers/overview30.pdf. [cit. 2025-03-12]

DOI 10.13164/juniorstav.2025.26138